Original Article

Cite This: Colloid & Nanoscience Journal 1 (2023) 130-138.

CNJ.araku.ac.ir

Synthesis and Characterization of New Nanocomposites Based on Poly(urethane-imide)s Reinforced Functionalized Carbone Nanotubes Containing N-Trimellitimido-L-Valine as Rigid Segments

Khalil Faghihi*[1], Masoumeh Soleimani[1], Mohammad Reza Enayat[1]

Received:2023-06-26
Revised: 2023-08-19
Accepted: 2023-08-19
DOI: **10.61186/CNJ.1.3.130**

[1]Organic Polymer Laboratory, Department of Chemistry, Faculty of Science, Arak University, Arak 38156-8-8349, Iran

Abstract

New poly(urethane-imide)s (PUIMs/MWCNT) nanocomposites (**8a** & **8b**) containing two different amounts of MWCNTs were prepared by *in situ* polymerization technique. We first prepared a new diisocyanate (**5)** containing imide moiety by a proper synthetic method. Then new poly(urethane-imide) (**7**) was prepared by reaction of diisocyanate (**5)** with hydroquinone and structure of resulting polymer was characterized by mean of FT-IR spectroscopy and elemental analysis. Also inherent viscosity of resulting poly(urethane-imide) (**7**) was measured about 0.35 dL/g. Transmission electron microscopy (TEM) showed that MWCNTs were exfoliated in the polymer matrix, resulting in well-dispersed morphologies at 1.5 and 2.5 mass% MWCNT contents. The effects of multiwall carbon nanotubes (MWCNT) on the thermal property of new PUIMs/MWCNT derived from diisocyanate (**5)** were investigated by thermogravimetric analysis (TGA) in nitrogen atmosphere. TGA results showed that the addition of MWCNT resulted a substantial increase of the thermal stability and char yields of the nanocomposites compared to the neat PUIMs. TEM experiments show morphology and good dispersion of nanotubes in polymeric matrix. The X-ray pattern of the PUIMs/MWCNT nanocomposites (**8a)** showed the combined peaks appearing in the MWCNT and pure PUIMs (**7**).

Keywords: Poly(urethane-imide)s, Carbon nanotube (CNTs), *In situ* polymerization

1. Introduction

Polymeric nanocomposites reinforced carbon nanotube (CNTs) have attracted wide scientific and industrial interests due to the varied impressive properties compared to pristine polymers. Polymers reinforced with carbon nanotubes have different applications in transportation applications, thermal management, and electronic and fuel cell. Good physical properties combined with high aspect ratio and unique nanostructures make carbon nanotube as useful reinforcements for high-performance and multifunctional polymer nanocomposites [1-5]. Polyurethanes (PUs) are multipurpose polymers. Unfortunately, they have low thermal stability, which limits their applications [6]. There are some efforts to improve the thermal stability of polyurethanes [5,7]. One way to improve the thermal stability of PU is the chemical modification of its structure by blending or copolymerizing with more thermally stable polymers. Poly(urethane-imide)s PUIMs are unique polymeric structures known for their interesting mechanical and thermal properties and also for their environmental friendly behaviors [5,8,9,10]. Incorporating symmetric aromatic imide rings with strong bonds into polyurethane backbone of PUIMs provide good balances between mechanical and thermal properties and flexibility of these materials [11,12].

However, for many applications, further improvements of the thermal or mechanical properties are still supposed to be desirable and carbon nanotubes (CNTs) are outstanding candidate reinforcing fillers. A great amount of research has been dedicated to the study and development of polymer-CNT nanocomposite materials with improved properties, since the discovery of CNTs in 1991. CNTs possess excellent mechanical, electrical, and thermal properties as well as nanometer scale diameter and high aspect ratio, which make them an ideal reinforcing agent for high strength polymer composites [4,13,14]. Polymers reinforced with CNTs have potential uses in different areas such as transportation applications, thermal management, electronics, and fuel cells [15]. In this article, two new PUIMs/MWCNT nanocomposites (**8a-b**) containing N-trimellitimido-L-valine as a rigid symmetry segment in the main chain were prepared via in situ technique. In the synthetic route we used multiwall carbon nanotubes (MWCNTs) particles, due to the cheap and convenient preparation of MWCNTs [16,17]. The effect of MWCNT on thermal properties of prepared nanocomposites was examined.

Corresponding Authors: Khalil Faghihi
k-faghihi@araku.ac.ir

2. Experimental

2.1. Materials

L-Alanine (99%), acetic acid (100%), HCl (36.5%), triethyl amine (99.5%), ethyl chloroformate (98%), sodium azide (99%), trimellitic anhydride (98%) and hydroquinone (99%) were purchased from Merck Chemical Co. (Germany) and also dibutyltin dilaurate (95%) was purchased from Fluka Chemical Co. (Switzerland). All solvents such as acetone, dimethyl formamide, benzene and methanol were purchased from Merck Chemical Co. (Germany) and used as laboratory grade.

2.2. Monomer Synthesis

2.2.1. N-Trimellitimido-L-valine (3)

N-Trimellitimido-L-valine (**3)** was prepared by a procedure reported elsewhere [18]. Into a 250 mL round-bottomed flask (10 mmol) of trimellitic anhydride (**1)**, (10 mmol) of L-Valine (**2)**, 80 mL of acetic acid and a stirring bar were placed. The mixture was stirred at room temperature for overnight and was refluxed for 4 hrs. The solvent was removed under reduced pressure and the residue was dissolved in 100 mL of cold water, then 5 mL of concentrated HCl was added. The solution was stirred until a white precipitate was formed, then the precipitate filtered off and dried, to give white crystals of diacid (**3)**: $[\alpha]_D^{25}$ = +128.9 (0.05 g in 10 mL DMF); mp= 208-210, FT-IR (KBr): 3430 (m), 2970 (m), 1775 (w, sh), 1709 (s, br), 1390 (s), 1199 (s), 1068 (w), 775 (w), 700 (w) cm^{-1}. ^{1}H-NMR (300 MHz, DMSO-d_6, δ, ppm): 13.8 (s, br, 2H). 7.8-8.2 (m, 3H), 4.8 (s, 1H), 2.2 (m, 1H), 1.2-1.4 (d, 3H), 0.80–0.85 (d, 3H). Elem. Anal. Calcd. For $C_{14}H_{13}NO_6$ (291.07): C, 57.73; H, 4.50; N, 4.81. Found: C, 57.30; H, 4.40; N, 4.70.

2.2.2. N-Trimellitimido-L-valine diisocyanate (5)

To a suspension of diacid (**3**) (4 mmol) and triethylamine (9.6 mmol) in acetone (15 mL), ethyl chloroformate (8.8 mmol) was slowly added at 0 °C. The resulting solution was stirred at 0 °C for 1 h and then a solution of NaN_3 (64 mmol) in water (80 mL) was slowly added at 0 °C. The solution was stirred for 3 h at 0 °C and then a mixture of ice and water (60 mL) was added until a white brown precipitate of N-trimellitimido-L-valine diacyl azide (**4**) was formed. The resulting precipitate was washed three times with distilled water and dried under vacuum. Then, a mixture of diacyl azide (**4**) (4 mmol) in dry benzene (75 mL) was refaxed for 8 h and the solvent was removed under vacuum conditions until a white brown solid of N-trimellitimido-L-valine diisocyanate **(5)** (yield: 84%) was formed (Scheme 1).

2.3. Polymer Synthesis

2.3.1. Preparation of PUIMs (7)

Into a 100-mL three-necked round-bottom flask, a solution of diisocyanate (**5)** (4 mmol) was added to dry DMF (30 mL) under N_2 atmosphere. Then, a solution of hydroquinone (**6)** (4 mmol) in dry DMF (25 mL) and a proper amount of dibutyltin dilaurate (0.2% by weight of the reactants) were added to diisocyanate solution as catalyst. The resulting mixture was heated at 80 °C for 12 hrs. By adding methanol (40 mL) as a non-solvent to the mixture, a white solid powder of PUIMs **(7)** was obtained (Scheme 1). The resulting product was filtered and dried under vacuum at 80 °C for 24 h (yield: 82%).

2.3.2. Preparation of PUIMs/MWCNT nanocomposite 8a, 8b by *in situ* technique

Appropriate amounts of MWCNT were dispersed in DMF under ultrasonication for half an hour. Hydroquinone (**6)** (4 mmol) was then added and stirred for 30 min, and a solution of diisocyanate (**5)** (4 mmol) in dry DMF (30 mL) under N_2 atomosphere was added under N^2 purged with vigorous stirring for 12h at room temperature. After the preparation of the PUIMs/MWCNT, the films were prepared by casting PUIMs/MWCNT solution onto glass plates for multistep thermal curing processes (30 min at 80 ˚C, 2 h at 120 ˚C and 2h at 160 ˚C). The PUIMs/MWCNT (**8a-b**) with two different loadings of CNT (1.5 and 2.5 mass%) were prepared.

2.4. Characterization

^{1}H-NMR spectra were recorded on a Bruker 300 MHz instrument (Germany). Fourier transform infrared (FTIR) spectra were recorded on Galaxy series FTIR 5000 spectrophotometer (England). Spectra of solids were performed using KBr pellets. Vibrational transition frequencies are reported in wave number (cm^{-1}). Band intensities are assigned as weak (w), medium (m), shoulder (sh), strong (s) and broad (br). Thermal Gravimetric Analysis (TGA) data for polymers were taken on a Mettler TA4000 System under N_2 atmosphere at a rate of 10 ˚C/min. The X-ray diffraction (XRD) patterns were recorded using a Philips X-pert diffractometer (CuKa radiation, k ¼ 0.15405 nm). The morphology of nanocomposites was investigated with a Philips A CM30 Transmission electron microscope.

3. Results and Discussion

3.1. Monomer synthesis

N-Trimellitimido-L-valine (**3)** was prepared by a one-step reaction as shown in Scheme 1. This compound was synthesized by the condensation reaction of one equimolar of trimellitic anhydride (**1)** with one equimolar of L-valine in acetic acid solution. Dissolving the residue in cold water gives a gummy like solid that breaks by adding concentrated HCl and gave a white color solid. The chemical structure and purities of diacid (**3)** were also analyzed by elemental analysis, ^{1}H-NMR and FTIR spectroscopy. The measured results in elemental analyses closely corresponded to the calculated ones, demonstrating that the expected compound was obtained. The ^{1}H-NMR spectrum of imide-acid (**3)** was shown in figure 1. The peak relevant to O-H carboxylic acid groups appeared at 13.8 ppm. Peaks at 7.8-8.2 ppm were assigned to the aromatic protons, peak at 4.4 ppm as singlet was assigned to the chiral carbon, peak appeared at 2.2 ppm was assigned to H-isopropyl group and two separated peaks at 1.2-1.4 and 0.8-0.9 ppm was assigned to methyl groups.

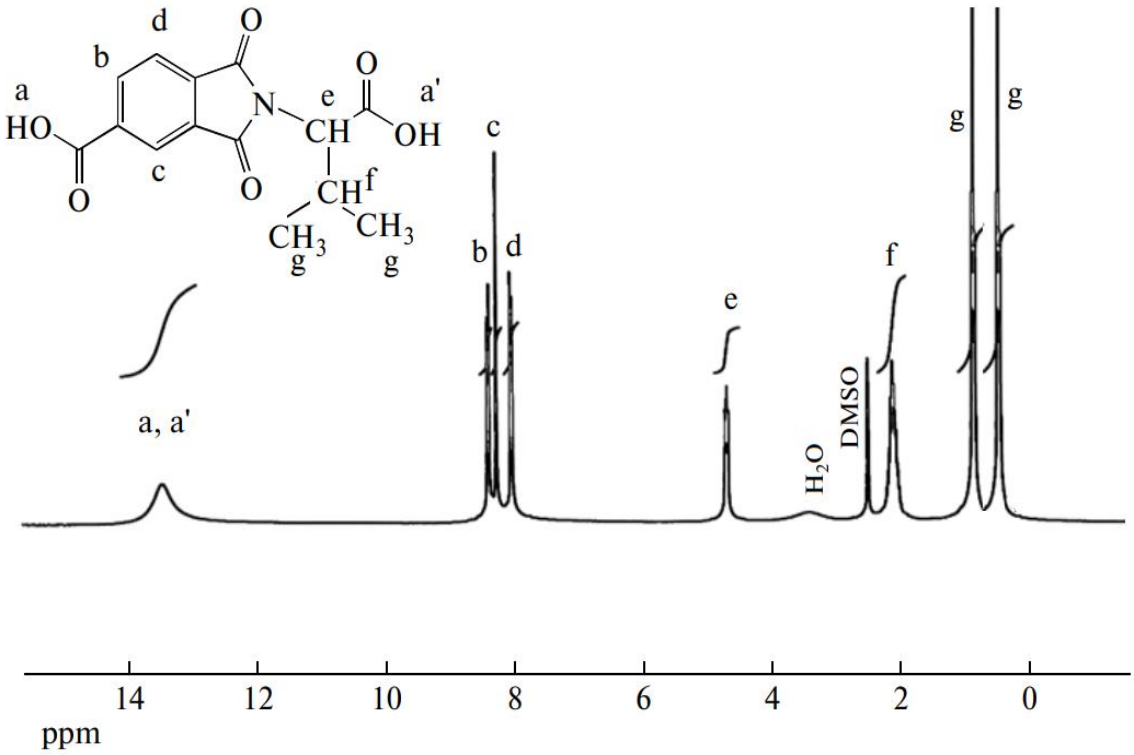

Fig. 1. ^{1}H-NMR of imide- acid 3

Fig. 2 displays FTIR of imide-acid (**3**), acyl-azide (**4**) and Diisocyante (**5**). In the FTIR of imide-acid (**3**) peaks appearing at 2800-3200 cm^{-1} (acid O-H stretching), 1775 and 1709 cm^{-1} (asymmetric and symmetric imide stretching), 1390 and 700 cm^{-1} (imide characteristic ring vibration) confirmed the presence of imide ring and carboxylic groups in this compound.

Imide-acid (**3**) was converted to the corresponding acyl-azide (**4**) as intermediate by reaction with ethyl chloroformate, triethyl amine, and sodium azide (Scheme 1). The FTIR spectrum of acyl azide (**4**) in figure 2 shows a new peak appearing at 2133 cm^{-1} which is related to acyl azide moiety. The obtained acyl azide (**4**) was converted to diisocyanate (**5**) through Curtius rearrangement by heating benzene as the solution. The FTIR spectrum of diisocyanate (**5**) in figure 2 also shows a new strong peak appearing at 2263 cm^{-1} which is related to isocyanate moiety.

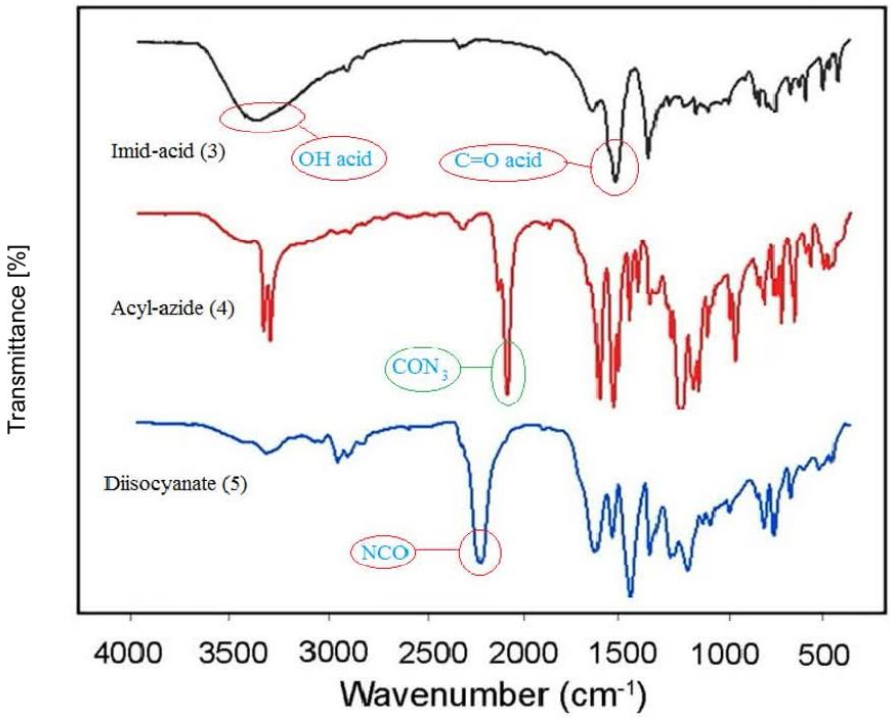

Fig. 2. FTIR of imide-acid (**3**), acyl-azide (**4**) and Diisocyante (**5**)

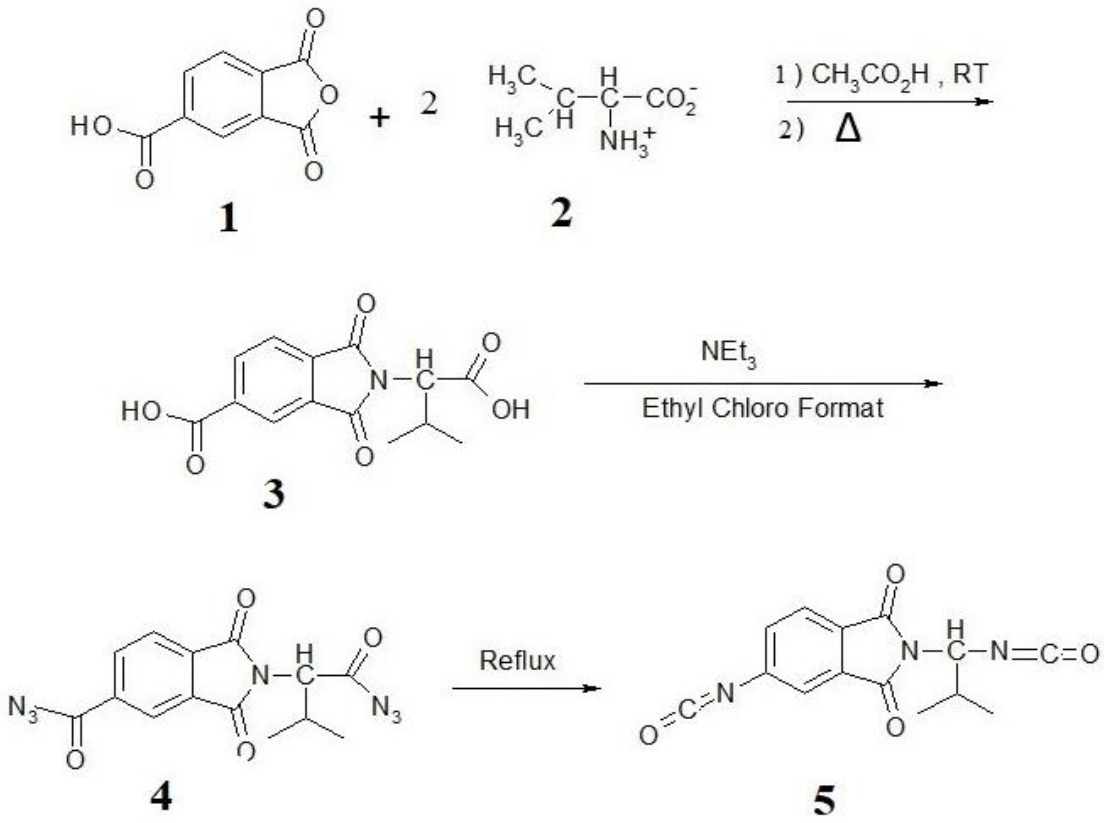

Scheme 1. Preparation of Diisocyanate 5

3.2. Polymer synthesis and characterization

PUIMs **(7)** containing imide symmetric segments and urethane linkages was synthesized by direct polycondensation reaction of with hydroquinone (**6)**, in the presence of dibutyltin dilaurate as catalysis in dry DMF as shown in Scheme 2.

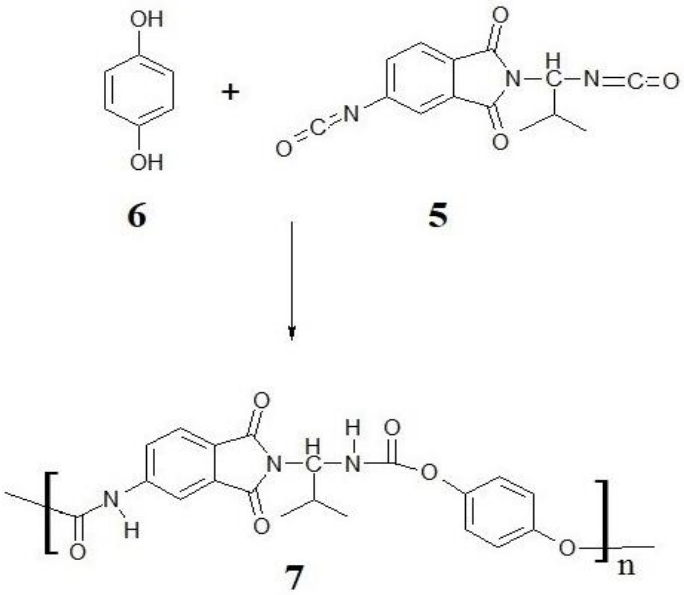

Scheme 2. Preparation of PUIMs 7

Resulting polymer was formed as cream powder with inherent viscosity about 0.35 dL/g and resulting date show we prepare a new polyurethane with moderate numerical molecular weight around 10^4 g/mol [19, 20]. The structure of prepared polymer was confirmed as poly(urethane-imide)s PUIMs by mean of FT-IR spectroscopy and elemental analysis. The structure of the resulting PUIMs (**7**) was confirmed using FTIR analysis. The FTIR spectrum showed that the main peak at 2263 cm^{-1} corresponding to isocyanate moiety disappeared and a new peak appeared at 1676 cm^{-1} which was related to urethane moiety (Fig. 3). The absorption bands at 1770 and 1712 cm^{-1} (asymmetric and symmetric C=O stretching vibration), 1371 and 718 cm^{-1} (imide characteristic ring vibration) show the presence of symmetry imide segments in polymer backbone.

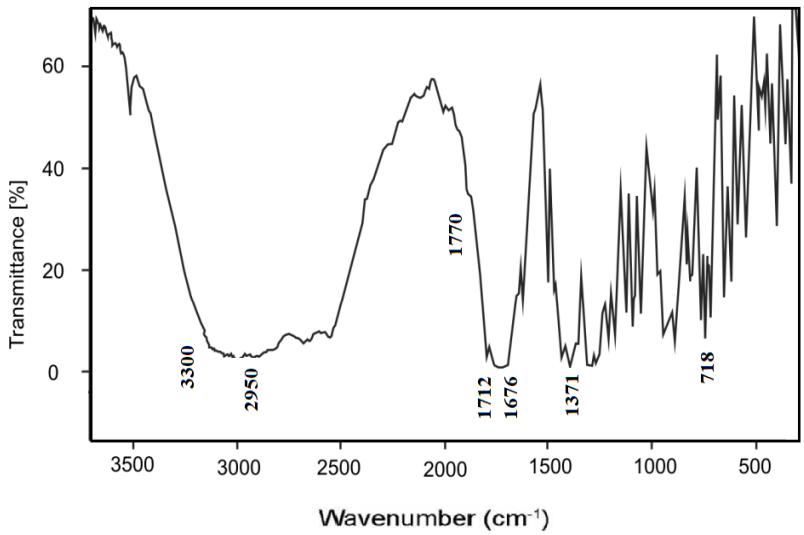

Fig. 3. FTIR of PUIMs 7.

The solubility of **PUIMs (7)** was investigated as 0.01 g of polymeric sample in 2 ml solvent. Polymer (7) is soluble in organic solvents such as DMF, DMSO and is insoluble in solvents such as chloroform, methylene chloride, methanol, ethanol and water.

3.3. Synthesis and characterization of PUIMs/MWCNT Nanocomposite 8a, 8b

Preparation of PUIMs/MWCNT nanocomposites was performed by in situ technique. Two different amounts of MWCNT were mixed with hydroquinone and the mixture was dispersed in DMF, under stirring and ultrasonic irradiation (Scheme 3).

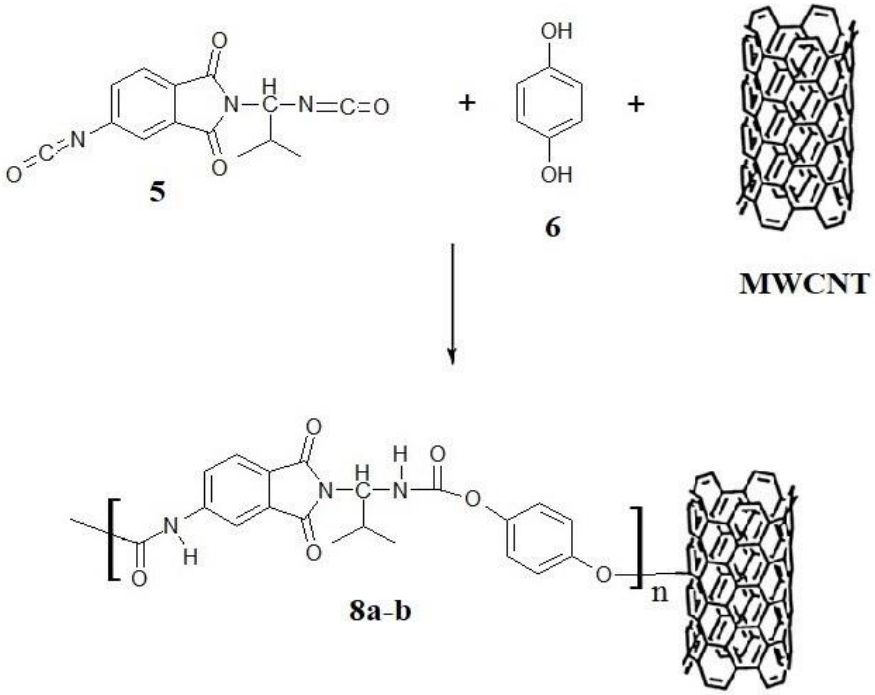

Scheme 3. Prararation of PUIMs/MWCNTs **8a-b.**

3.4. TEM images

TEM experiments show morphology and dispersion of nanotubes in polymeric matrix. The dispersion of MWCNT in the PUIMs matrix generally depends on level of interactions between Nano fillers and polymer matrix. To observe the bulk morphological structure of PUIMs/MWCNT nanocomposites samples, TEM imaging from nanocomposites containing 1.5 and 2.5 mass% MWCNT at two magnifications have been carried out and shown in Fig. 4. It can be seen that MWCNT is well dispersed within the PUIMs matrix even at higher MWCNT loadings. It can explain by the fact that the MWCNT stabilizes their dispersion by good interactions with the PUIMs matrix. The presences of the high amount of imide groups in the polymer backbone can result in the interfacial interaction between the polymer matrix and the CNTs in the nanocomposites.

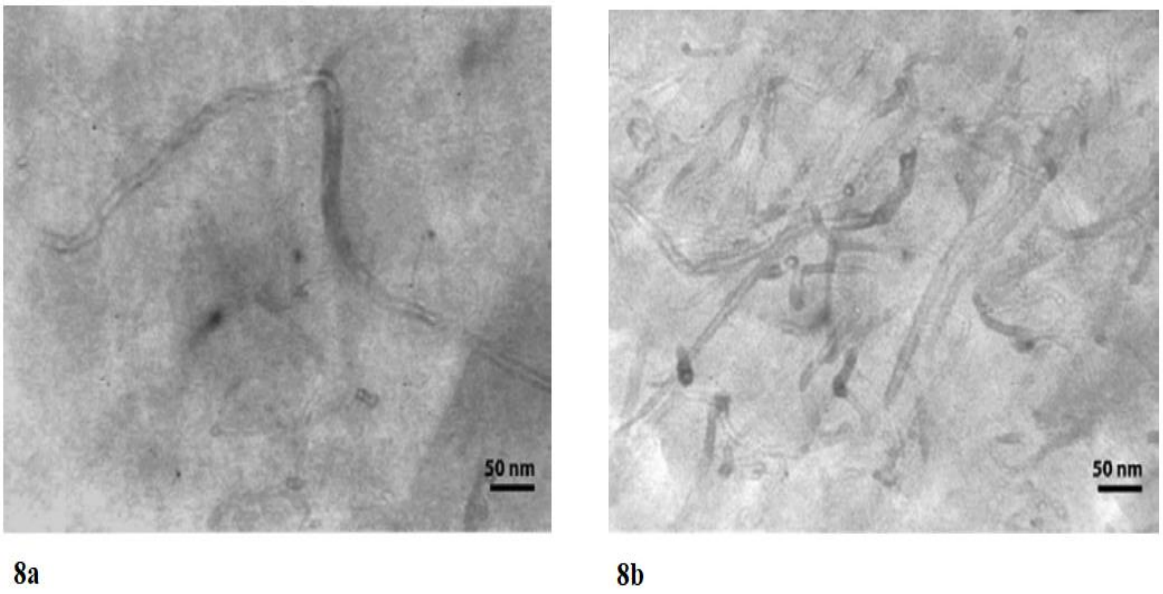

Fig. 4. PUIMs/MWCNT Nanocomposite 8a, 8b.

3.5. XRD analysis

To study the structure of the PUIMs/MWCNT nanocomposites, X-ray diffraction measurement was

carried out (Fig. 5). The X-ray patterns of the MWCNT displayed the presence of two peaks at 25.7 and 44.3. PUIMs showed a broad diffraction peak at 10–30, which indicated that PUIMs is amorphous. The X-ray pattern of the PUIMs/MWCNT nanocomposites nanocomposite 1.5 wt% showed the combined peaks appearing in the MWCNT and pure PUIMs. The position of the peaks corresponding to the two constituents of the nanocomposite was same to the individual of PUIMs and MWCNT, which illustrated that either the orientation of the PUIMs chains or the structure of MWCNTs was not, influenced each other during the process of preparation.

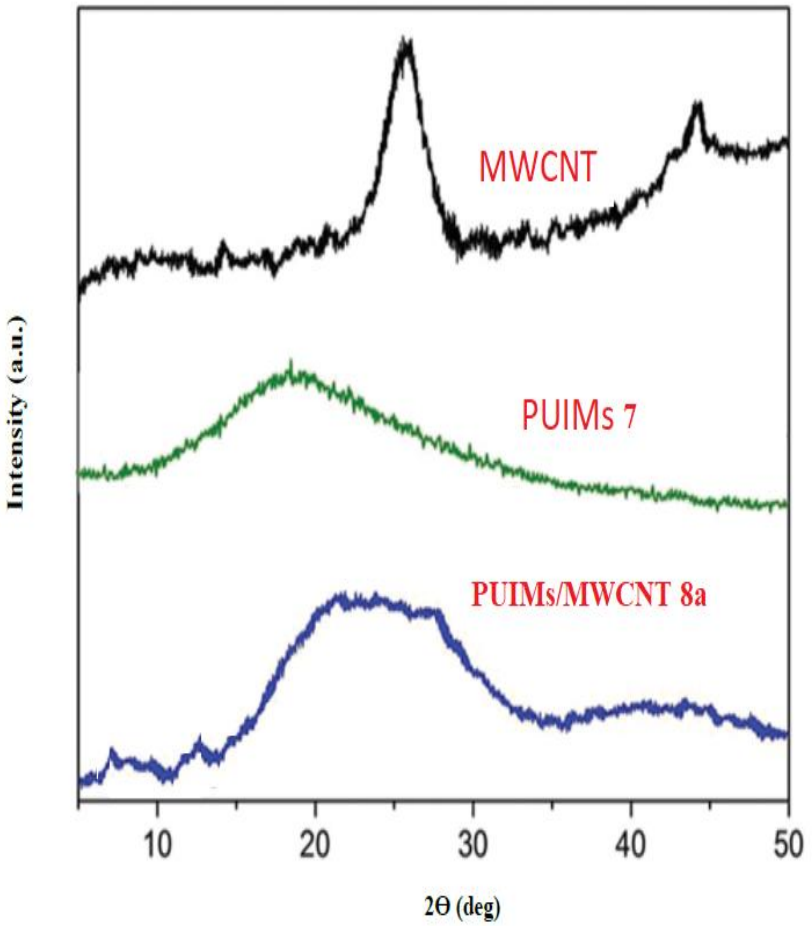

Fig. 5. XRD patterns of MWCNT, PUIMs and PUIMs/MWCNT 1.5 wt%.

3.6. Thermal properties

The thermal properties of PUIMs (**7**) and their nanocomposites (**8a-b**) have been characterized under nitrogen atmosphere at heating rate of 10 ^{0}C min^{-1}. TG curves of the samples in nitrogen are shown in Fig. 6 while the corresponding data are summarized in Table 1. The TG data in nitrogen indicate that PUIMs (**7**) and their nanocomposite (**8a)** and (**8b)** containing imide and urethane moieties possess enhanced thermal stability compare to simple polyurethane. The pristine PUIMs show initial mass loss in nitrogen at 287 ^{0}C. Results show after MWCNT addition; the thermal stability of the materials increases in comparison with pristine PUIMs. With respect to the char residue of the samples at 500 ^{0}C, they leave more than 40 % char yield in nitrogen. The high char yield of samples in nitrogen may be associated with their high aromatic content. Especially, PUIMs /MWCNT (**8b)** show the highest residue yield up to 46.3 %. With the increasing MWCNT contents, the degradation temperature shifts up. By incorporating MWCNTs into the polymeric matrix, the thermal stability of polymers can be enhanced. More complete MWCNT exfoliation might hold the key to the present observation of the high polymer carbon nanotube thermal stability. The results confirm good dispersion of MWCNT even at higher concentration.

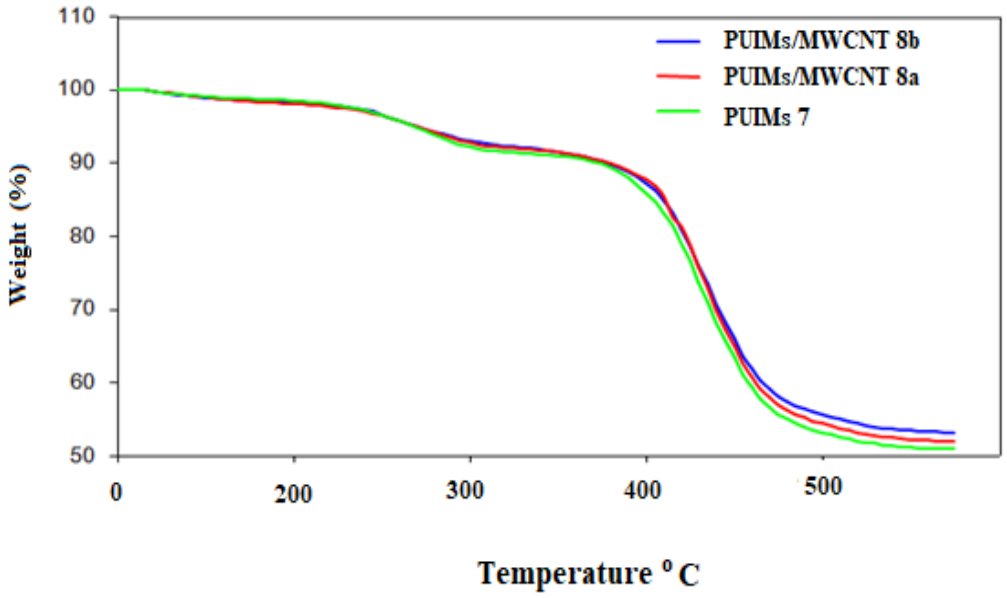

Fig. 6. TGA data of PUIMs 7 & PUIMs/MWCN 8a, 8b.

Table 1. Thermal behavior of PUIMs **7** and PUIMs/MWCT **8a**, **8b**

polymer	T_5(˚C)[a]	T_{10}(˚C)[b]	Char yield [c]
7	287	310	40.0
8a	295	315	43.4
8b	297	323	46.3

[a,b] Temperature at which 5% or 10% weight loss was recorded by TGA at a heating rate of 10˚C/min under N_2. [c] Weight percentage of material left after TGA analysis at a maximum temperature of 500˚C under N_2.

4. Conclusions

The present work has shown that N-trimellitimido-L-valine (**3)** is an interesting monomer which contains both hard imide linkage and soft aliphatic isopropyl segment. This compound was converted to diisocyanate (**5**) by two steps reaction. Diisocyanate (**5**) same imide-iacid (**3**) has two different segments and is proper for preparation poly(urethane-imide) (**7**) by reaction with hydroquinone (**6**). As we mentioned before polyurethanes have wide applications in industry but has a main drawback and usually show low thermal stability. Also PUIMs/MWCNT nanocomposites (**8a-b**) were successfully prepared via a simple in situ polymerization process followed by casting with a heating program. TEM results have revealed homogenous dispersion of MWCNTs within the PUIMs matrix. The addition of MWCNTs into a PUIMs matrix led to obvious improvements in the thermal properties of nanocomposites comparing with neat PUIMs, especially for PUIMs/MWCNT (**8b**).

Conflicts of Interest

The author declares no conflict of interest.

Author information

*Corresponding Author: Khalil Faghihi
E-mail address: k-faghihi@araku.ac.ir

ORCID
Khalil Faghihi: 0000-0001-9884-1788

References

[1] D. G. Papageorgiou, Z. Li, M. Liu, I. A. Kinloch and R. J. Young ,Mechanisms of mechanical reinforcement by graphene and carbon nanotubes in polymer nanocomposites, Nanoscale. 12 (2020) 2228-2267. https://doi.org/10.1039/C9NR06952F

[2] A. Iqbal, A. Saeed & A. Ul-Hamid, A review featuring the fundamentals and advancements of polymer/CNT nanocomposite application in aerospace industry, Polym. Bull. 78 (2021) 539–557. https://doi.org/10.1007/s00289-019-03096-0

[3] A. Salabat, F. Mirhoseini, Polymer-based nanocomposites fabricated by microemulsion method, Polym. Compos. 43 (2022) 1282–94. https://doi.org/10.1002/pc.26504
[4] P. Y. Li, Q. Wang, S. Wang, A review on enhancement of mechanical and tribological properties of polymer composites reinforced by carbon nanotubes and graphene sheet: Molecular dynamics simulations, Comp. Part B: Eng. 160 (2019) 348-361. https://doi.org/10.1016/j.compositesb.2018.12.026.
[5] H. Eibagi & K. Faghihi, Preparation of thermally stable magnetic poly(urethane-imide) /nanocomposite containing β-cyclodextrin cavities as new adsorbent for lead and cadmium, Polym. Res. 27(301) (2020). https://doi.org/10.1007/s10965-020-02255-6
[6] P. Liu, Q. Zhang, L. He, Q. Xie, H. Ding, Thermal and mechanical properties of poly(urethane-imide)/epoxy/silica hybrids, Wil. InterSci. (2010). https://doi.org/10.1002/app.32322
[7] F. Kamali, K. Faghihi, F. Mirhoseini, High antibacterial activity of new eco-friendly and biocompatible polyurethane nanocomposites based on Fe_3O_4/Ag and starch moieties. Polymer Eng. Sci., 62(5) (2022) 1444-1462.https://doi.org/10.1002/pen.25934
[8] M. Albozahid, H. Z. Naji, Z. K. Alobad, J. K. Wychowaniec, A. Saiani, Synthesis and characterization of hard copolymer polyurethane/functionalized graphene nanocomposites: Investigation of morphology, thermal stability, and rheological properties, App. Polym. Sci. 139(45) (2022). https://doi.org/10.1002/app.53118
[9] A. Kairyte, S. Cztonka, D. S. Ducike and S. Vejelis, Impact of sunflower press cake and its modification with liquid glass on polyurethane foam composites: thermal stability, ignitability, and fire resistance, Polym. 14(21) (2022) 4543. https://doi.org/10.3390/polym14214543
[10] C. L. Lin, W. L. Lin & S. P. Rwei, Synthesis and characterization of poly(urethane-imide) derived from structural effect of diisocyanates, Polym. Res. 30(54) (2023). https://doi.org/10.1007/s10965-022-03408-5
[11] Y. Guo, A. M. Cristadoro, J. Kleemann, S. Bokern, R. P. Sijbesma, and Z. Tomovic, Solvent-free preparation of thermally stable poly(urethane-imide) elastomers, ACS Appl. Polym. Mater. 5(6) (2023) 4517–4524. https://doi.org/10.1021/acsapm.3c00626
[12] M. Meena, A. Kerketta, M. Tripathi, P. Roy, J. Jacob, Thermally stable poly(urethane-imide)s with enhanced hydrophilicity for waterproof-breathable textile coatings, App. Polym. Sci. 139(28) (2022). https://doi.org/10.1002/app.52508
[13] N. M. Nurazzi, F. A. Sabaruddin, M. M. Harussani, S. H. Kamarudin, M. Rayung, M. R. M. Asyraf, H. A. Aisyah, M. N. F. Norrrahim, R. A. Ilyas, N.Abdullah, E. S. Zainudin, S. M. Sapuan and A. Khalina, Mechanical performance and applications of cnts reinforced polymer composites- a review, Nanomat. 11(9) (2021) 2186. https://doi.org/10.3390/nano11092186
[14] S. T. Vegas, A. Muhsan, C. Liu, M. Tarfaoui and K. Lafdi, The Effect of Agglomeration on the Electrical and Mechanical properties of polymer matrix nanocomposites reinforced with carbon nanotubes, Polym. 14(9) (2022) 1842. https://doi.org/10.3390/polym14091842
[15] A. H. Muhammad Ismail, F. M. AL-Oqla, M. S. Risby & S. M. Sapuan, On the enhancement of the fatigue fracture performance of polymer matrix composites by reinforcement with carbon nanotubes: a systematic review, Carb. Lett. 32 (2022) 727-740. https://doi.org/10.1007/s42823-022-00323-z
[16] W. Xia, Y.-H. Feng, J. Zou, J. Huang, M.-M. Guo, P. Zhang, Low percolation conductive graphite flakes-filled poly(urethane-imide) composites with high thermal stability via imidization self-foaming structure, Mater. Chem. 21 (2021) 100516. https://doi.org/10.1016/j.mtchem.2021.100516
[17] L.N. Saw, M. Mariatti, A.R. Azura, A. Azizan, J.K. Kim, Transparent, electrically conductive, and flexible films made from multiwalled carbon nanotube/epoxy composites, Comp. Part B: Eng. 43(8) (2012) 2973-2979. https://doi.org/10.1016/j.compositesb.2012.05.048
[18] M. Hajibeygi, K. Faghihi, and M. Shabanian, Preparation and characterization of new photosensitive and optically active poly(amide_imide)s from *n*_trimellitylimido_*l*_amino acid and dibenzalacetone moiety in the main chain, poly. Sci. Ser. B, 53 (2011) 518–527. https://doi.org/10.1134/S1560090411090016
[19] D.-J. Liaw, F.-C. Chang, J.-H. Liu, K.-L. Wang, K. Faghihi, S.-H. Huang, K.-R. Lee, J.-Y. Lai, Novel thermally stable and chiral poly(amide-imide)s bearing from N,N0-(4,40-diphthaloyl)-bis-L-isoleucine diacid: Synthesis and characterization, Poly. Deg. and Sta. 92 (2007) 323-329. https://doi.org/10.1016/j.polymdegradstab.2006.10.005
[20] D.-J. Liaw, F.-C. Chang, J.-H. Liu, K.-L. Wang, K. Faghihi, K.-R. Lee, J.-Y. Lai, Synthesis and Characterization of Novel Thermally Stable and Optically Active Poly(amide-imide)s Derived from N,N0-(4,40-Diphthaloyl)-bis-L-leucine Diacid and Aromatic Diamines, App. Polym. Sci. 104 (2007) 3096–3102. https://doi.org/10.1163/138577210X12634696333271